

# Toward High-Performance Polymer Photovoltaic Devices for Low-Power Indoor Applications

Shun-Shing Yang, Zong-Chun Hsieh, Muchamed L. Keshtov, Ganesh D. Sharma, and Fang-Chung Chen\*

This article describes the performance of organic photovoltaic (OPV) devices, incorporating three different polymer/fullerene derivative blends, under low-level lighting conditions. The devices exhibit much higher power conversion efficiencies (PCEs) under indoor lighting conditions than they do under sunlight. The best-performing device is capable of delivering a power output of  $22.57 \mu\text{W cm}^{-2}$ , corresponding to a PCE of 13.76%, under illumination with indoor lighting conditions at 500 lux. Increasing the open-circuit voltage ( $V_{oc}$ ) of the OPV devices is the most critical factor for achieving high device performance for low-power indoor applications. Therefore, the device power output will be maximized if we could obtain a larger energy difference between the highest occupied molecular orbital of the polymer donor and the lowest unoccupied molecular orbital of the electron acceptor, thereby ensuring a high value of  $V_{oc}$ .

## 1. Introduction

Shrinking the size and decreasing the power consumption of electronic devices has enabled many new functions and will lead to many new future applications. Many predict that a new technological revolution will arise from the development of the Internet of Things (IoT).<sup>[1,2]</sup> The IoT is a system in which various physical objects (“things”) are connected through a giant internet capable of exchanging data among the things, sensing their environments, and responding to their external stimuli. The IoT has significant potential to benefit a variety of fields, including home automation, security, and surveillance; healthy monitoring; and building power management.<sup>[1,2]</sup> Such a smart system will,

however, require an enormous power supply. Distributed harvesters of energy from the local environment could be particularly critical for improving the efficiency and sustainability of the whole energy-system provider. Moreover, because the IoT would contain a huge number of wireless sensors, controls, and active electronic components (e.g., actuators, devices, displays), off-grid power sources that operate with high efficiencies and high energy densities would play important roles.

Many methodologies have been proposed for harvesting energy from local environments, including vibration/motion energy, thermoelectricity, and photovoltaics.<sup>[3,4]</sup> Among these technologies, photovoltaic energy has great promise because of its high energy density and relatively

high output voltage.<sup>[5]</sup> In particular, several emerging photovoltaic technologies, including organic photovoltaics (OPVs),<sup>[5–9]</sup> dye-sensitized solar cells (DSSCs)<sup>[5,6,10]</sup> and organic/inorganic hybrid perovskite solar cells,<sup>[11]</sup> might become efficient energy sources for harvesting low-level lighting. In 2015, Mori et al. studied the performance of OPV devices under irradiation with light-emitting diodes (LEDs) and compared the device parameters with those of crystal silicon solar cells. They predicted that a power conversion efficiency (PCE) of 21.3% could be obtained under daylight color LED illumination.<sup>[8]</sup> More recently, Cutting et al. reported that OPV devices, which exhibited PCEs much lower than those of Si solar cells when measured under the conventional AM1.5G standard, could surpass Si cells – with higher measured PCEs – under LED illumination.<sup>[9]</sup> Considering their many other attractive properties (e.g., light weight, flexibility, low cost), OPVs have great potential to open up a variety of new indoor or low-level lighting applications that have not been possible when using Si solar cells.

Although highly efficient OPV devices that operate under low-level lighting conditions have been demonstrated, further improvement will be necessary if they are to compete with other photovoltaic technologies. Nevertheless, very few systematic investigations have been made of the device characteristics and physics and of the relevant properties of the electronic organic materials required to improve the device performance under low-power indoor illumination conditions. In this study, we evaluated the potential of polymer photovoltaic devices to be used in low-power lighting applications. We applied two artificial light sources – an inorganic LED and a fluorescent tube (FT) – to

S. S. Yang, Z. C. Hsieh, Prof. F. C. Chen  
Department of Photonics  
National Chiao Tung University  
Hsinchu 30010, Taiwan  
E-mail: fcchen@mail.nctu.edu.tw

Prof. M. L. Keshtov  
Institute of Organoelement Compounds of the Russian Academy of Sciences  
Moscow 119991, Russian Federation

Prof. G. D. Sharma  
Department of Physics  
The LNM Institute of Information Technology  
Jamdoli, Jaipur, Rajasthan 302031, India

 The ORCID identification number(s) for the author(s) of this article can be found under <https://doi.org/10.1002/solr.201700174>.

DOI: 10.1002/solr.201700174

examine the performance of the photovoltaic devices under indoor illumination conditions. We investigated several polymer blends as photoactive layers. Impressive performance occurred under illumination with the artificial lighting. The photovoltage was the most important determinant of high efficiency; the photocurrent was less critical, because these state-of-the-art device architectures already possessed high capability to harvest photons within the relatively narrow visible spectral range of the existing artificial light sources. We believe that our results might open up new directions for further improving the device performance of OPV devices for local energy harvesters under low-power lighting applications.

## 2. Experimental Section

OPV devices were prepared on indium tin oxide (ITO)-coated glass substrates.<sup>[12]</sup> The substrates were cleaned sequentially with a detergent, deionized water, acetone, and isopropanol. After further drying in an oven for at least 12 h, the ITO substrates were treated with UV-ozone for 15 min. The anodic buffer, poly(3,4-ethylenedioxythiophene):polystyrenesulfonate (PEDOT:PSS), was deposited on top of the ITO surface through spin-coating and then the resulting sample was baked at 120 °C for 1 h. The photoactive layer, comprising a conjugated polymer and a fullerene derivative, was spin-coated onto the PEDOT:PSS-coated substrates. The polymer blends included regioregular poly(3-hexylthiophene) (P3HT):[6,6]-phenyl-C<sub>61</sub>-butyric acid methyl ester (PC<sub>60</sub>BM), P3HT:indene-C<sub>60</sub>

bisadduct (ICBA), and poly[4,8-bis(5-(2-ethylhexyl)thiophen-2-yl)benzo[1,2-b;4,5-b']dithiophene-2,6-diyl-*alt*-(4-(2-ethylhexyl)-3-fluorothieno[3,4-*b*]thiophene)-2-carboxylate-2,6-diyl)] (PBDTTT-EFT):[6,6]-phenyl-C<sub>71</sub>-butyric acid methyl ester (PC<sub>70</sub>BM). **Figure 1** presents the chemical structures and energy levels of these materials. The weight ratios of P3HT:PC<sub>60</sub>BM, P3HT:ICBA, and PBDTTT-EFT:PC<sub>70</sub>BM in the active layers were 1:1, 1:0.6, and 1:1.5, respectively. Additives were blended into the polymer blends to enhance the device efficiencies. 1-Chloronaphthalene (CN; 3%, v/v) was added into both the P3HT:PC<sub>60</sub>BM and P3HT:ICBA devices.<sup>[13]</sup> Similarly, diiodohexane (DIH; 4%, v/v) was blended into the PBDTTT-EFT:PC<sub>70</sub>BM devices.<sup>[14]</sup> To complete each device, a bilayer cathode was deposited through sequential thermal evaporation of Ca (30 nm) and Al (100 nm) under vacuum. The devices were encapsulated with cover glasses using UV-curable epoxy before testing. Photocurrent density–voltage (*J*–*V*) characteristics were measured using a Keithley 2400 source measure unit. The device performance was measured under illumination from either an AM1.5 solar simulator (100 mWcm<sup>-2</sup>), a white LED (SY 674, Sheng Yih Technologies), or a FT (TL5, Philips). **Figure 2** displays the emission spectra of the LED and FT. The color temperatures of the LED and FT were 5000 and 6500 K, respectively. The light intensity of the solar simulator was calibrated using a standard Si photodiode equipped with a KG-5 filter (Hamamatsu). The illuminance of each artificial light source was measured using a light meter (TES Electrical Electronic Corp., 1339R). The light power was also measured by using a Si detector (UDT Instruments). External quantum

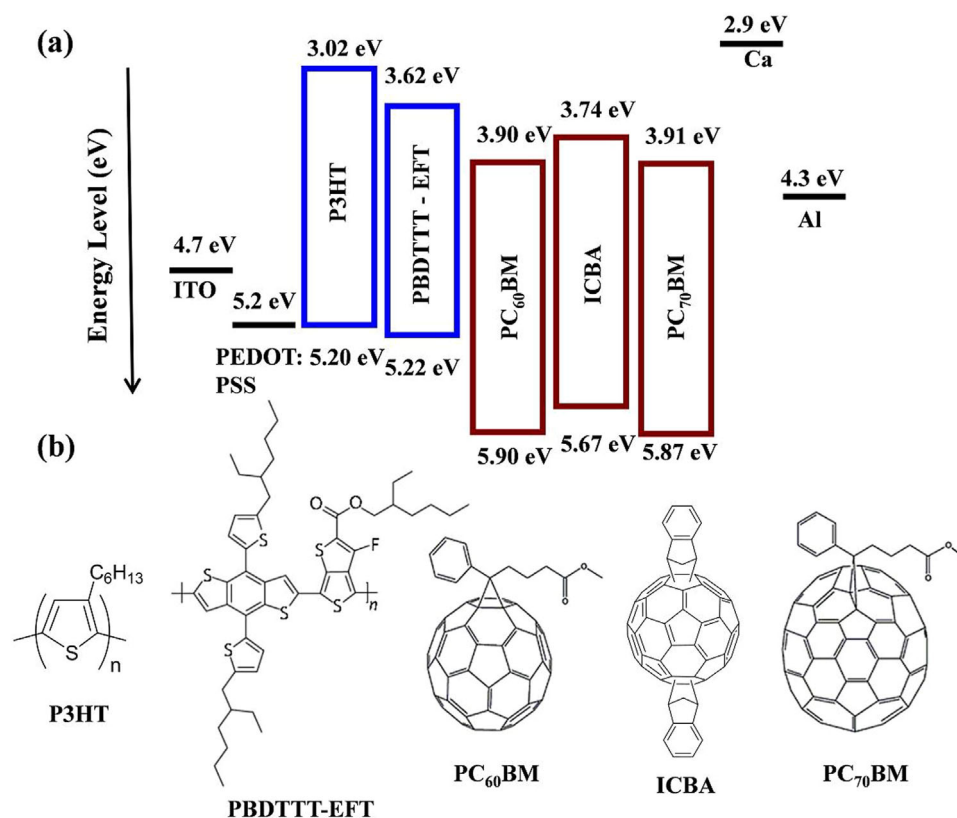


**Figure 1.** a) Energy level diagram of the organic materials used in this study. b) Chemical structures of the materials.

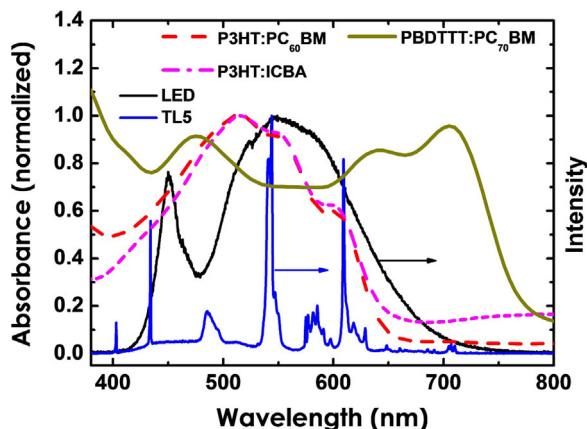


**Figure 2.** Emission spectra of the two artificial light sources (inorganic LED; TL5 FT) and absorption spectra of the three different polymer/fullerene derivative blends: P3HT:PC<sub>60</sub>BM, P3HT:ICBA, and PBDTTT-EFT:PC<sub>70</sub>BM.

efficiency (EQE) spectra were recorded using an Enli system. All measurements were made in air.

### 3. Results and Discussion

Figure 3(a) presents the current density–voltage ( $J$ – $V$ ) characteristics of the three kinds of OPV device under illumination at  $100 \text{ mW cm}^{-2}$  (AM 1.5G). The P3HT:PC<sub>60</sub>BM device prepared with CN as the additive exhibited an open-circuit voltage ( $V_{oc}$ ) of 0.61 V, a short-circuit current density ( $J_{sc}$ ) of  $9.92 \text{ mA cm}^{-2}$ , and a fill factor (FF) of 0.64, resulting in a PCE of 3.86%. The value of  $V_{oc}$  of the P3HT:ICBA device was relatively higher, at 0.89 V; thus, the PCE improved to 4.90%, even though the value of  $J_{sc}$  had decreased to  $8.20 \text{ mA cm}^{-2}$ . The device featuring the low band gap (LBG) polymer PBDTTT-EFT also exhibited superior device performance because it could absorb photons of longer wavelength from the solar irradiation (Figure 2).<sup>[15]</sup> The PCE of the PBDTTT-EFT:PC<sub>70</sub>BM-containing device was 6.95%. Table 1 summarizes the electrical properties of the OPV devices obtained under illumination at 1 sun.

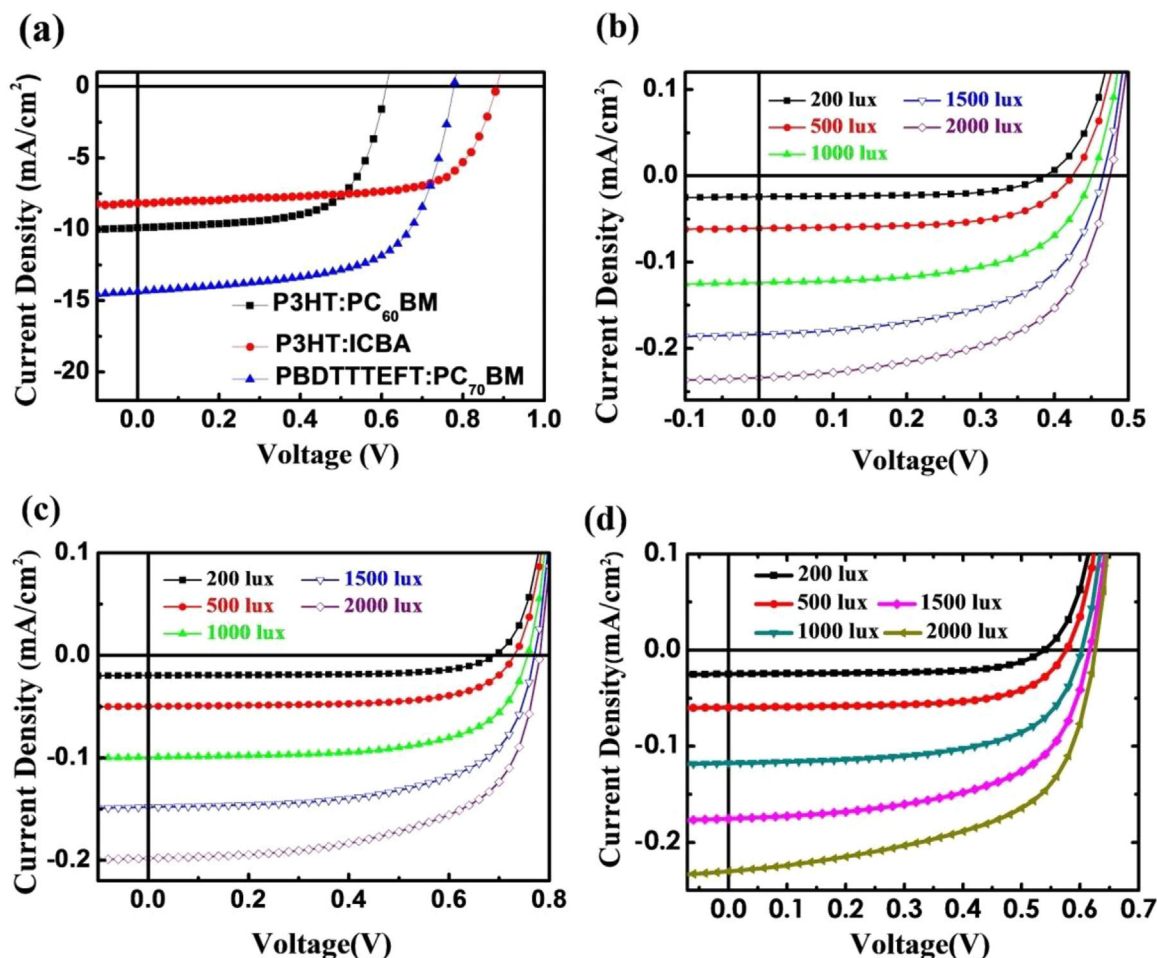


**Figure 3.** a)  $J$ – $V$  curves of the various OPV devices obtained under illumination of 1 sun ( $100 \text{ mW cm}^{-2}$ , AM1.5G). b–d)  $J$ – $V$  curves of the OPV devices recorded under illumination from a TL5 fluorescent tube at various illuminances; photoactive layers: (b) P3HT:PC<sub>60</sub>BM, (c) P3HT:ICBA, and (d) PBDTTT-EFT:PC<sub>70</sub>BM.

**Table 1.** Electrical characteristics of devices under illumination of 1 sun.

Device	$V_{oc}$ (V)	$J_{sc}$ ( $\text{mA cm}^{-2}$ )	FF	PCE (%)
P3HT:P <sub>60</sub> CBM	0.59 ± 0.01	9.66 ± 0.14	0.65 ± 0.01	3.68 ± 0.07
P3HT:ICBA	0.89 ± 0.01	8.20 ± 0.12	0.67 ± 0.01	4.90 ± 0.07
PBDTTT-EFT:PC <sub>70</sub> BM	0.75 ± 0.01	14.52 ± 0.17	0.63 ± 0.03	6.95 ± 0.27

Two major differences exist between sunlight and light from indoor lighting sources. The first is the light intensity. The power intensity of the AM1.5G standard is  $100 \text{ mW cm}^{-2}$ ; the intensity of the indoor lighting sources typically ranges from 0.5 to  $1 \text{ mW cm}^{-2}$  – that is, a factor 100–500 lower.<sup>[9]</sup> Accordingly, the photovoltaic devices would display much lower power output under indoor conditions. The second difference is the spectral range. While sunlight covers a very broad spectral range, from the ultraviolet to the infrared, indoor lighting sources usually emit photons within the visible range only (Figure 2). Therefore, it should be easier to design photovoltaic devices that exhibit a photoresponse over such a narrow range.

Indeed, these OPV devices exhibited much better performance when illuminated with the artificial light sources. Figure 3(b) and (c) present the  $J$ – $V$  characteristics of the three kinds of OPV devices under illumination with light from the TL5 fluorescent tube at various illuminances. Figure S1, Supporting Information displays the corresponding performance of the OPV devices under illumination with light from the LED. Although the values of  $V_{oc}$  and  $J_{sc}$  were relatively low, the device based on P3HT:P<sub>60</sub>CBM typically exhibited PCEs greater than 9% when irradiated with light from the TL5 fluorescent tube; these PCEs were higher than those measured under illumination of 1 sun, suggesting that this OPV device could harvest photon energy from the TL5 FT more efficiently. In addition, Figure 2 reveals that the P3HT:P<sub>60</sub>CBM thin films could indeed harvest most of the photons emitted from the FT.

After the electron acceptor was replaced by ICBA, the values of  $V_{oc}$  increased; for example, to 0.77 V at 500 lux – a lighting level typical of heavily used offices.<sup>[9]</sup> We attribute the higher value of  $V_{oc}$  and larger PCE to the higher energy level of the lowest unoccupied molecular orbital (LUMO) of ICBA (Figure 1),<sup>[16,17]</sup> thereby minimizing energy loss upon exciton separation at the donor–acceptor interfaces. Therefore, although the photocurrent decreased slightly compared with that of the P3HT:PC<sub>60</sub>BM-based

device, the overall PCE still increased to 13.76%. Tables S1–S6, Supporting Information summarize the electrical characteristics of all the OPV devices, measured under illumination with the two artificial light sources at various light intensities. Interestingly, the device performances under illumination from the two light sources were very similar, suggesting that the narrow ranges of visible wavelengths of the lighting emissions were almost covered by the organic materials examined in this study.

Figure 3(c) reveals that the PBDTTT-EFT:PC<sub>70</sub>BM-based device also displayed much better performance under illumination from the TL5 fluorescent tube. The PCEs were generally greater than 12% in the range of illumination intensities, reaching 13.14% at 500 lux – comparable with the behavior of the P3HT:ICBA device. A close examination of the performances of the devices incorporating P3HT:ICBA and PBDTTT-EFT:PC<sub>70</sub>BM (Table 2 and Tables S3–S6, Supporting Information) indicated that the former provided higher values of  $V_{oc}$  but the latter had a higher photocurrent. Their photovoltages were relative to the energy difference between the highest occupied molecular orbitals (HOMOs) of the polymer donor and the lowest unoccupied molecular orbitals (LUMOs) of fullerene acceptors (1.31 eV); that of the PBDTTT-EFT:PC<sub>70</sub>BM-based device was smaller (1.46 eV), resulting in lower values of  $V_{oc}$ . Table S7, Supporting Information further summarizes the representative device performance for dim-light applications, including DSSCs, OPVs, perovskite solar cells and the results of this work.

Although PBDTTT-EFT had a lower band gap, the value of  $J_{sc}$  of its device was only slightly larger than that of the P3HT:PC<sub>60</sub>BM-based device (Table 2), suggesting very similar absorption abilities for the two devices. Figure 4 compares the EQE spectra of the three different devices; the overlap of these spectra and the emission spectra of the two artificial light sources was almost identical for the P3HT:PC<sub>60</sub>BM- and PBDTTT-EFT:PC<sub>70</sub>BM-containing devices, further confirming their similar photocurrents. These observations suggested relatively limited room for further improvements in the values of  $J_{sc}$ . Therefore, the photovoltage was presumably rather more critical for determining the performance of OPV devices under illumination from artificial lighting sources. Although the P3HT:ICBA-based device exhibited lower photocurrents because of its relatively low EQEs, it still had a very high power output because of less “loss-in-potential” (the difference between the value of  $V_{oc}$  and the band gap of the polymer). This finding is consistent with

**Table 2.** Electrical characteristics of devices under illumination from two artificial light sources at 500 lux.

Device	Light source	$V_{oc}$ (V)	$J_{sc}$ ( $\text{mA cm}^{-2}$ )	FF	PCE (%)	$P_{out}^a$ ( $\mu\text{W cm}^{-2}$ )
P3HT:P <sub>60</sub> CBM	TL5	0.43 ± 0.01	0.062 ± 0.001	0.59 ± 0.01	9.59 ± 0.15	15.77 ± 0.24
	LED	0.43 ± 0.01	0.062 ± 0.001	0.59 ± 0.01	8.90 ± 0.14	15.67 ± 0.22
P3HT:ICBA	TL5	0.73 ± 0.01	0.050 ± 0.001	0.62 ± 0.03	13.76 ± 0.60	22.57 ± 0.98
	LED	0.73 ± 0.01	0.050 ± 0.001	0.63 ± 0.01	13.05 ± 0.42	22.97 ± 0.73
PBDTTT-EFT:PC <sub>70</sub> BM	TL5	0.58 ± 0.01	0.063 ± 0.002	0.59 ± 0.04	13.14 ± 0.26	21.56 ± 0.40
	LED	0.59 ± 0.01	0.066 ± 0.003	0.58 ± 0.04	13.20 ± 0.17	23.23 ± 1.07

<sup>a)</sup> Maximum energy output.

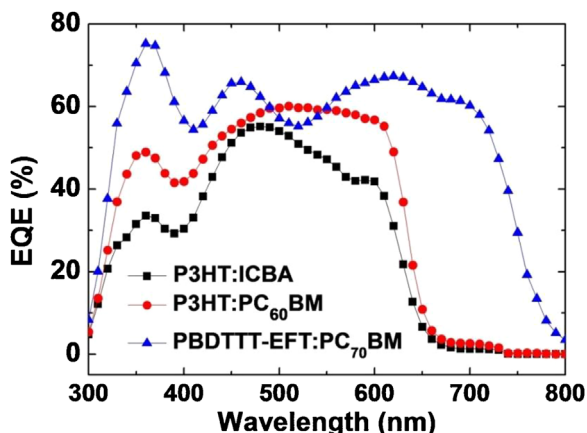


**Figure 4.** EQE spectra of the three OPV devices as displayed in Figure 3(a).

a prediction made previously – that increasing the value of  $V_{oc}$  would be necessary to obtain high PCEs from OPV devices operated indoors.<sup>[8]</sup> Therefore, we conclude that even higher PCEs might be achieved if we could design a polymer having a low-lying HOMO to increase the value of  $V_{oc}$ .

Next, we investigated the dependence of the value of  $J_{sc}$  on the lighting power. As displayed in Figure 5(a), the values of  $J_{sc}$  were roughly proportional to the light intensity ( $L$ ). We fitted the data using the equation<sup>[18]</sup>

$$J \propto L^a \quad (1)$$

where  $J$  is the short-circuit current density and  $a$  is the determined exponential factor. The values of  $a$  for the P3HT: P<sub>60</sub>CBM-, P3HT:ICBA-, and PBDTTT-EFT:PC<sub>70</sub>BM-based devices were 0.88, 0.86, and 0.90, respectively, under illumination with solar irradiation at various intensities; they increased to 0.95, 1.00, and 0.98, respectively, under illumination from the TL5 FTs at various intensities. The higher values of  $a$  suggest lower levels of charge recombination and/or limited space charge effects under indoor lighting conditions as a result of lower photocurrents in these devices.<sup>[18,19]</sup> Thus, these OPV devices appear to be very suitable for indoor applications, because the lower charge densities under lower-power illumination ensure efficient charge transport and a lower tendency for charge recombination.<sup>[20]</sup> Notably, the slopes of the lines in Figure 5(a) depended on the type of light source used for illumination, probably because of the better light harvesting ability from artificial light sources.

Figure 5(b) displays the dependence of the values of  $V_{oc}$  upon the light intensity of the OPV devices. The values of  $V_{oc}$  can be expressed using the equation<sup>[7]</sup>

$$V_{oc} = \frac{nkT}{q} \ln \left( \frac{I_{ph}}{I_s} + 1 \right) \cong \frac{nkT}{q} \ln \left( \frac{I_{ph}}{I_s} \right) \propto \ln(I_{ph}) \quad (2)$$

where  $n$  is the ideality factor of the diode,  $k$  is the Boltzmann constant,  $T$  is the temperature,  $q$  is the elementary charge, and  $I_{ph}$  and  $I_s$  are the photocurrent and saturation current, respectively. Under normal operating conditions, the saturation

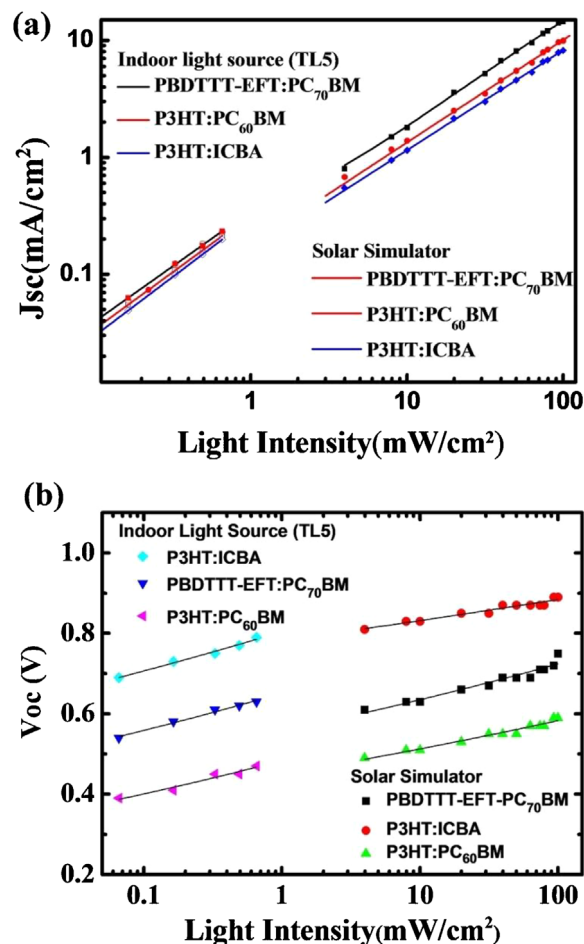


**Figure 5.** Dependence of the values of (a)  $J_{sc}$  and (b)  $V_{oc}$  of the OPV devices on the intensity of the incident light. The lines are corresponding fitting curves.

current is very small compared with the value of  $I_{ph}$ . Therefore, the value of  $V_{oc}$  is approximately proportional to the logarithm of the photocurrent. Because we had previously demonstrated the near-linear relationship between the value of  $I_{ph}$  and the light intensity [Figure 5(a)], we deduce that the value of  $V_{oc}$  exhibited a logarithmic dependence upon the light intensity. Indeed, Figure 5(b) reveals the logarithmic dependences of the values of  $V_{oc}$  on the light intensity for illumination under both sunlight and a TL5 FT. The slopes of these curves were almost identical, suggesting that the logarithmic dependence would be valid for polymer blends having various band gaps. In other words, the tendency for decreasing photovoltage upon decreasing light intensity would be similar among the polymer blends.

We also note that the values of  $V_{oc}$  for the devices under illumination from artificial lighting sources were almost equal to or even slightly higher than the ones obtained under from solar irradiation [Figure 5(b)]. For example, the  $V_{oc}$  of the PBDTTT-EFT:PC<sub>70</sub>BM device was 0.63V at ca. 0.7 mW cm<sup>-2</sup>, which was higher than that (0.61 V) of the device illuminated at 4 mW cm<sup>-2</sup> with solar irradiation. The detailed reason is still unclear. We suspect, however, that it might be due to different emission spectra of the two light sources and different level of charge

recombination. Because of the higher PCEs, the level of charge recombination within the device could be lower.

The other interesting observation is that the FF values were usually larger while they were obtained under solar irradiation (Tables 1 and 2). In fact, we could somehow observe the FF values decreased with the decreasing light intensity; Figure S2, Supporting Information revealed one typical example. We suspect that the traps within the active layers might be filled at a high illumination intensity, resulting in lower values of FF. More studies, however, should be further performed to support this argument.

A typical IoT sensor node requires an energy input in the sub-milliwatt regime.<sup>[21]</sup> A credit card-sized cell (ca. 45 cm<sup>2</sup>) would deliver power of ≈1 mW under illumination at 500 lux, suggesting that OPV devices are a feasible technology for indoor-power applications. In other words, our study has proven that OPV devices are indeed suitable for IoT technologies. With further improvements in device performance (e.g., lowering the HOMO energy level of the polymer's electron donors), we may harvest more power locally for additional indoor applications.

#### 4. Conclusions

We have investigated the performance of OPV devices made of various polymer/fullerene derivatives under low-level lighting conditions. The PCEs of the devices were much higher under indoor lighting conditions than they were under sunlight. They also exhibited very similar behavior under illumination with light from both a white LED and a TL5 FT. The best-performing device delivered a power output of 22.57 μW cm<sup>-2</sup>, corresponding to a PCE of 13.76% under illumination at 500 lux. Our study suggests that increasing the value of  $V_{oc}$  of OPV devices is the decisive factor for achieving high PCEs for indoor applications; because the state-of-art OPV devices could readily cover the narrow emission range of the artificial light sources, the values of  $J_{sc}$  were easier to optimize (i.e., there is only relatively limited room for further improvements in photocurrent). We have found that the greater value of  $V_{oc}$  resulting when using an electron acceptor having a higher LUMO energy level greatly improved the device performance under low-power lighting conditions. We anticipate that the PCE could be improved further by increasing the energy gap between the HOMO of the donor (conjugated polymer) and the LUMO of the acceptor (fullerene). For example, a polymer possessing a low-lying HOMO energy level should lead to a higher value of  $V_{oc}$  and, thereby, a higher PCE.

#### Supporting Information

Supporting Information is available from the Wiley Online Library or from the author.

#### Acknowledgments

We thank the Ministry of Science and Technology of Taiwan (grants MOST 105-2119-M-492-001, MOST 104-2221-E-009-094-MY3, and MOST 103-2923-E-009-001-MY3) and the Ministry of Education of Taiwan (through the ATU program) for financial support.

#### Conflict of Interest

The authors declare no conflict of interest.

#### Keywords

indoor, internet of things, photovoltaic, polymers

Received: October 19, 2017

Published online: November 8, 2017

- [1] I. C. L. Ng, S. Y. L. Wakenshaw, *Int. J. Res. Mark.* **2017**, *34*, 3.
- [2] L. D. Xu, W. He, S. Li, *IEEE Trans. Industr. Inform.* **2014**, *10*, 2233.
- [3] R. M. Ferdous, A. W. Reza, M. F. Sustain, *Energy Rev.* **2016**, *58*, 1114.
- [4] J. A. Paradiso, T. Starner, *IEEE Pervasive Comput.* **2005**, *4*, 18.
- [5] M. Freunek, M. Freunek, L. M. Reindl, *IEEE J. Photovolt.* **2013**, *3*, 59.
- [6] B. Minnaert, P. Veelaert, *Energies* **2014**, *7*, 1500.
- [7] R. Steim, T. Ameri, P. Schilinsky, C. Waldauf, G. Dennler, M. Scharber, C. J. Barbec, *Sol. Energy Mater. Sol. Cells* **2011**, *95*, 3256.
- [8] S. Mori, T. Gotanda, Y. Nakano, M. Saito, K. Todori, M. Hosoya, *Jpn. J. Appl. Phys.* **2015**, *54*, 071602-1.
- [9] C. L. Cutting, M. Bag, D. Venkataraman, *J. Mater. Chem. C* **2016**, *4*, 10367.
- [10] A. Fakharuddin, R. Jose, T. M. Brown, F. Fabregat-Santiago, J. Bisquert, *Energy Environ. Sci.* **2014**, *7*, 3952.
- [11] C. Y. Chen, J. H. Chang, K. M. Chiang, H. L. Lin, S. Y. Hsiao, H. W. Lin, *Adv. Funct. Mater.* **2015**, *25*, 7064.
- [12] F. C. Chen, C. J. Ko, J. L. Wu, W. C. Chen, *Sol. Energy Mater. Sol. Cells* **2010**, *94*, 2426.
- [13] F. C. Chen, H. C. Tseng, C. J. Ko, *Appl. Phys. Lett.* **2008**, *92*, 103316.
- [14] M. S. Su, C. Y. Kuo, M. C. Yuan, U. Jeng, C. J. Su, K. H. Wei, *Adv. Mater.* **2011**, *23*, 3315.
- [15] W. Huang, E. Gann, L. Thomsen, C. Dong, Y. B. Cheng, C. R. McNeill, *Adv. Energy Mater.* **2015**, *5*, 1401259-1.
- [16] Y. He, H. Y. Chen, J. Hou, Y. Li, *J. Am. Chem. Soc.* **2010**, *132*, 1377.
- [17] J. L. Wu, F. C. Chen, M. K. Chuang, K. S. Tan, *Energy Environ. Sci.* **2011**, *4*, 3374.
- [18] J. L. Wu, F. C. Chen, Y. S. Hsiao, F. C. Chien, P. Chen, C. H. Kuo, M. H. Huang, C. S. Hsu, *ACS Nano* **2011**, *5*, 959.
- [19] V. D. Mihalevich, H. X. Xie, B. de Boer, L. J. A. Koster, P. W. M. Blom, *Adv. Funct. Mater.* **2006**, *16*, 699.
- [20] S. Y. Kok, Z. C. Hsieh, C. H. Chou, S. S. Yang, M. K. Chuang, Y. T. Lin, S. S. Yap, T. Y. Tou, F. C. Chen, *Sci. Adv. Mater.* **2017**, *9*, 1435.
- [21] W. S. Wang, T. O'Donnell, N. Wang, *ACM J. Emerg. Technol. Comput. Syst.* **2010**, *6*, 6-1.